

## Electrical Conductivities, Viscosities, and Densities of *N*-Methoxymethyl- and *N*-Butyl-*N*-methylpyrrolidinium Ionic Liquids with the Bis(fluorosulfonyl)amide Anion

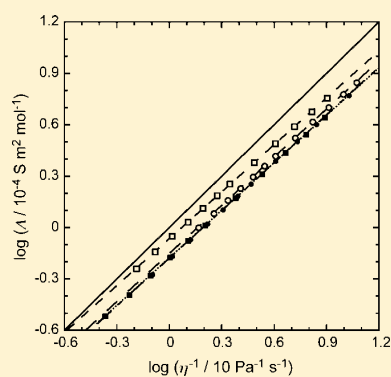
Takashi Makino,<sup>†</sup> Mitsuhiro Kanakubo,<sup>\*,†</sup> Tatsuya Umecky,<sup>†</sup> Akira Suzuki,<sup>†</sup> Tetsuo Nishida,<sup>‡</sup> and Jun Takano<sup>‡</sup>

<sup>†</sup>National Institute of Advanced Industrial Science and Technology (AIST), 4-2-1 Nigatake, Miyagino-ku, Sendai 983-8551, Japan

<sup>‡</sup>Research and Development Department, Stella Chemifa Corporation, 1-41 Rinkai-cho, Izumiotsu, Osaka 595-0075, Japan

### Supporting Information

**ABSTRACT:** This paper reports the densities, viscosities, and electrical conductivities of the two pyrrolidinium ionic liquids, *N*-methoxymethyl-*N*-methylpyrrolidinium bis(fluorosulfonyl)amide ([Pyr<sub>1,101</sub>][FSA]) and *N*-butyl-*N*-methylpyrrolidinium bis(fluorosulfonyl)amide ([Pyr<sub>1,4</sub>][FSA]), over the temperature range  $T = (273.15 \text{ to } 363.15) \text{ K}$  at atmospheric pressure. The densities were fitted to polynomials, and the viscosities and electrical conductivities were analyzed with the Vogel–Fulcher–Tammann and Litovitz equations. The densities and electrical conductivities of [Pyr<sub>1,101</sub>][FSA] are higher than those of [Pyr<sub>1,4</sub>][FSA], while the viscosities of the former salt are smaller than those of the latter. The Walden plots (double logarithm graph of molar conductivity vs fluidity (reciprocal viscosity)) give the straight lines with the slopes being 0.91 to 0.94. The present results for [Pyr<sub>1,101</sub>][FSA] and [Pyr<sub>1,4</sub>][FSA] are compared with those for the bis(trifluoromethanesulfonyl)amide ([NTf<sub>2</sub>]<sup>−</sup>) analogues, [Pyr<sub>1,101</sub>][NTf<sub>2</sub>] and [Pyr<sub>1,4</sub>][NTf<sub>2</sub>].



## INTRODUCTION

Room temperature ionic liquids (ILs) are salts, the melting points of which are at or below ambient temperatures. They generally consist of a large asymmetric cation and an organic or inorganic anion. ILs have some favorable characters: negligible vapor pressure, nonflammability, high thermal and chemical stability, a wide electrochemical window, high solubility of certain specific gases, and so on. Because of these features, ILs have attracted much attention, for example, as electrolytes in batteries, solvents for chemical reactions, and media for separation processes. An understanding of the nature of ILs is of importance for related technologies; therefore, a large number of investigations have been performed on the physical and chemical properties of ILs. Pyrrolidinium-based ILs, a kind of aliphatic quaternary ammonium ILs, have widely been studied because they are considered as promising candidates for Li secondary batteries.<sup>1–9</sup> Additionally, ILs with bis(fluorosulfonyl)amide anion ([FSA]<sup>−</sup>) have shown more attractive properties (higher electrical conductivities and lower viscosities) than corresponding ILs with bis(trifluoromethanesulfonyl)amide ([NTf<sub>2</sub>]<sup>−</sup>).<sup>1–4</sup>

Our research group has measured accurately the densities, viscosities,<sup>10–12</sup> and electrical conductivities<sup>13,14</sup> of imidazolium-based ILs as a function of temperature and pressure. In addition, such properties of *N*-methoxymethyl-*N*-methylpyrrolidinium bis(trifluoromethanesulfonyl)amide ([Pyr<sub>1,101</sub>][NTf<sub>2</sub>]) and *N*-butyl-*N*-methylpyrrolidinium bis(trifluoromethanesulfonyl)amide ([Pyr<sub>1,4</sub>][NTf<sub>2</sub>]) have been recently investigated over a wide range of temperatures at atmospheric pressure.<sup>15,16</sup> In the present study, the densities, viscosities, and

electrical conductivities of two different pyrrolidinium salts with the [FSA]<sup>−</sup> anion, *N*-methoxymethyl-*N*-methylpyrrolidinium bis(fluorosulfonyl)amide ([Pyr<sub>1,101</sub>][FSA]), and *N*-butyl-*N*-methylpyrrolidinium bis(fluorosulfonyl)amide ([Pyr<sub>1,4</sub>][FSA]) have been measured over the temperature range  $T = (273.15 \text{ to } 363.15) \text{ K}$  at atmospheric pressure. In addition, the present results have been compared with those of analogues pyrrolidinium-based ILs with the [NTf<sub>2</sub>]<sup>−</sup> anion ([Pyr<sub>1,101</sub>][NTf<sub>2</sub>] and [Pyr<sub>1,4</sub>][NTf<sub>2</sub>]).

## EXPERIMENTAL SECTION

**Materials.** [Pyr<sub>1,4</sub>][FSA] (purity: > 99 %, water: <~30 ppm) was purchased from PIOTREK Co., Ltd. [Pyr<sub>1,101</sub>][FSA] (purity: > 99 %, water: ~8 ppm) was prepared at Stella Chemifa Co., Ltd. as follows: a 31 g aliquot of chloromethyl methyl ether (Tokyo Chemical Industry, reagent-grade) was slowly added with stirring to approximately 30 cm<sup>3</sup> toluene solution of 30 g of *N*-methylpyrrolidine (Tokyo Chemical Industry, reagent-grade) cooled in an ice bath, and the mixture was then refluxed at 333 K for 8 h. The mixture was filtered and dried under reduced pressure, and about 50 g of the solid product, *N*-methoxymethyl-*N*-methylpyrrolidinium chloride ([Pyr<sub>1,101</sub>][Cl]), was obtained. Potassium bis(fluorosulfonyl)amide, K[FSA], was prepared according to the literature procedure.<sup>17</sup> To replace Cl<sup>−</sup> by [FSA]<sup>−</sup>, ~80 g [Pyr<sub>1,101</sub>][Cl] in

Received: August 2, 2011

Accepted: January 9, 2012

Published: February 2, 2012

aqueous solution (a water content was 80 g) was mixed with 106 g K[FSA] and stirred vigorously for 1 h. The upper aqueous phase was decanted and the lower IL layer washed with water several times and dried under reduced pressure. The chloride contents of aqueous solutions in contact with the samples were less than the detection limit of AgNO<sub>3</sub> testing. A sample of 105 g of colorless [Pyr<sub>1,101</sub>][FSA] was obtained. Any excess water in each IL was further removed by evacuation at 323 K for approximately 30 h just prior to measurements. Dried ILs were transferred to the closed electrical cell or instruments by use of an airtight syringe under dry nitrogen or argon. The water contents of [Pyr<sub>1,4</sub>][FSA] and [Pyr<sub>1,101</sub>][FSA] were (30 and 8)·10<sup>-6</sup> mass fractions, respectively, as determined by Karl Fischer titration.

**Apparatus and Procedure.** The instruments and the experimental equipments were the same as previously described elsewhere.<sup>15</sup> The densities were measured using a vibrating tube densimeter (Anton Paar, DMA 5000M). The built-in viscosity correction for this instrument was employed as previously confirmed by the references with known viscosities.<sup>10–12</sup> The instrumental constants were calibrated using dry air and distilled water, which was purified by a Millipore Simpli Lab Purification Pack. The viscosities were determined with a rotating-cylinder viscometer (Anton Paar, Stabinger SVM 3000). The reliability and validity of the viscosities were confirmed by measuring the reference samples supplied by Cannon Instrument Company as described in the previous study.<sup>15</sup> The impedance measurement was performed with an impedance analyzer (Bio Logic, SP-150). The solution resistance ( $R_{sol}$ ) was obtained from the Nyquist plot by fitting the measured impedances to the best-fit form of an arbitrary electric circuit. Both potentiometric and galvanometric procedures gave the same resistance within the experimental errors. A syringe-type cell with a pair of platinum electrodes was employed. The cell constant was 35.4 m<sup>-1</sup> at 298.15 K, and the correction for thermal expansion was made for different temperatures, as stated in the previous reports.<sup>13,14</sup> The sample temperature was kept within 0.01 K at most in all of the measurements. The expanded uncertainty for the densities is 0.05 kg·m<sup>-3</sup>, and those for the viscosities and electrical conductivities are less than 2 %.

## RESULTS AND DISCUSSION

The densities ( $\rho/\text{kg}\cdot\text{m}^{-3}$ ) at atmospheric pressure for [Pyr<sub>1,101</sub>][FSA] and [Pyr<sub>1,4</sub>][FSA] are summarized in Tables 1 and 2

**Table 1. Densities  $\rho$ , Viscosities  $\eta$ , Electrical Conductivities  $\kappa$ , and Molar Conductivities  $\Lambda$  of [Pyr<sub>1,101</sub>][FSA] from  $T = (273.15 \text{ to } 363.15) \text{ K}$  at Atmospheric Pressure**

$T$ K	$\rho$ kg·m <sup>-3</sup>	$\eta$ mPa·s	$\kappa$ S·m <sup>-1</sup>	$\Lambda$ μS·m <sup>2</sup> ·mol <sup>-1</sup>
273.15	1427.09	67.8 <sub>7</sub>	0.460	100.0
278.15	1422.56	55.6 <sub>9</sub>	0.554	120.9
283.15	1418.07	46.3 <sub>1</sub>	0.659	144.2
288.15	1413.61	39.0 <sub>0</sub>	0.772	169.6
293.15	1409.17	33.2 <sub>0</sub>	0.898	197.8
298.15	1404.75	28.5 <sub>0</sub>	1.03 <sub>3</sub>	228.2
303.15	1400.37	24.7 <sub>1</sub>	1.17 <sub>8</sub>	261.0
313.15	1391.69	19.0 <sub>7</sub>	1.49 <sub>2</sub>	332.8
323.15	1383.09	15.1 <sub>4</sub>	1.84 <sub>1</sub>	413.1
333.15	1374.59	12.2 <sub>4</sub>	2.22 <sub>2</sub>	501.8
343.15	1366.16	10.1 <sub>1</sub>	2.63 <sub>6</sub>	598.8
353.15	1357.81	8.48	3.06 <sub>8</sub>	701.2
363.15	1349.52	7.22		

**Table 2. Densities  $\rho$ , Viscosities  $\eta$ , Electrical Conductivities  $\kappa$ , and Molar Conductivities  $\Lambda$  of [Pyr<sub>1,4</sub>][FSA] from  $T = (273.15 \text{ to } 363.15) \text{ K}$  at Atmospheric Pressure**

$T$ K	$\rho$ kg·m <sup>-3</sup>	$\eta$ mPa·s	$\kappa$ S·m <sup>-1</sup>	$\Lambda$ μS·m <sup>2</sup> ·mol <sup>-1</sup>
273.15	1326.81	153.2	0.236	57.3
278.15	1322.77	120.5	0.295	71.9
283.15	1318.75	96.2 <sub>4</sub>	0.363	88.6
288.15	1314.76	78.0 <sub>5</sub>	0.439	107.7
293.15	1310.79	64.1 <sub>3</sub>	0.525	129.2
298.15	1306.86	53.2 <sub>4</sub>	0.619	152.7
303.15	1302.94	44.7 <sub>6</sub>	0.722	178.7
313.15	1295.18	32.7 <sub>2</sub>	0.959	238.8
323.15	1287.50	24.7 <sub>2</sub>	1.23 <sub>1</sub>	308.3
333.15	1279.89	19.1 <sub>9</sub>	1.53 <sub>8</sub>	387.4
343.15	1272.35	15.3 <sub>0</sub>	1.86 <sub>5</sub>	472.7
353.15	1264.88	12.4 <sub>3</sub>	2.23 <sub>0</sub>	568.3
363.15	1257.47	10.2 <sub>8</sub>		

and plotted against temperature in the Supporting Information (Figure S1). The experimental data were fitted to the following polynomials of temperature:

$$[\text{Pyr}_{1,101}][\text{FSA}]: (\rho/\text{kg}\cdot\text{m}^{-3}) \\ = 1707.80 - 1.15327(T/\text{K}) + 4.59221\cdot 10^{-4}(T/\text{K})^2 \quad (1)$$

$$[\text{Pyr}_{1,4}][\text{FSA}]: (\rho/\text{kg}\cdot\text{m}^{-3}) \\ = 1577.13 - 1.02691(T/\text{K}) + 4.04125\cdot 10^{-4}(T/\text{K})^2 \quad (2)$$

The standard errors for the coefficients in the equations were obtained as follows:  $\pm 0.97$ ,  $\pm 0.00615$ , and  $\pm 0.09688\cdot 10^{-4}$  in eq 1;  $\pm 0.93$ ,  $\pm 0.00590$ , and  $\pm 0.09289\cdot 10^{-4}$  in eq 2. The residuals (experimental data – calculated data) for the densities are shown in Figure 1. The calculated values are in good agreement

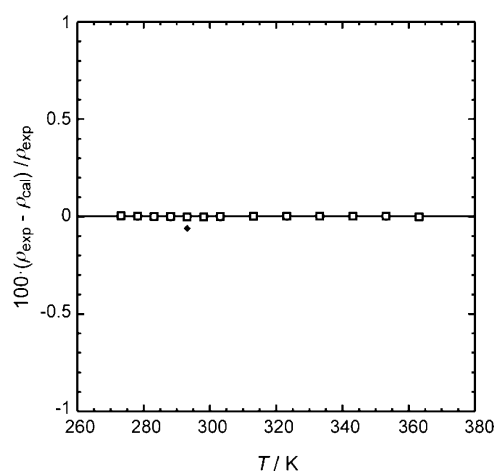


**Figure 1.** Residuals between the experimental density  $\rho_{exp}$  and the calculated density  $\rho_{cal}$  as a function of temperature  $T$ . Circle (open), [Pyr<sub>1,101</sub>][FSA]; square (open), [Pyr<sub>1,4</sub>][FSA]; diamond (filled), [Pyr<sub>1,4</sub>][FSA] (ref 4). Data points of [Pyr<sub>1,101</sub>][FSA] are covered with those of [Pyr<sub>1,4</sub>][FSA].

with the experimental values over the entire temperature range of the present study (less than  $\pm 0.005$  %). The density of [Pyr<sub>1,4</sub>][FSA] at 293.15 K agrees well with the reported value.<sup>4</sup> The densities of [Pyr<sub>1,101</sub>][FSA] are larger than those of [Pyr<sub>1,4</sub>][FSA]. The ILs with the [NTf<sub>2</sub>]<sup>-</sup> anion have larger

densities than those with the [FSA]<sup>-</sup> anion. Table 3 lists the molar volumes ( $V_m/\text{cm}^3\cdot\text{mol}^{-1}$ ) and expansion coefficients

**Table 3. Molar Volumes  $V_m$  and Expansion Coefficients  $\beta$  of the Pyrrolidinium-Based Ionic Liquids with [FSA]<sup>-</sup> and [NTf<sub>2</sub>]<sup>-</sup> Anions at 298.15 K**

	$V_m$	$\beta$	$V_m$	$\beta$	
	$\text{cm}^3\cdot\text{mol}^{-1}$	$10^{-4} \text{K}^{-1}$	$\text{cm}^3\cdot\text{mol}^{-1}$	$10^{-4} \text{K}^{-1}$	
[Pyr <sub>1,101</sub> ][FSA]	220.921	6.2605	[Pyr <sub>1,4</sub> ][FSA]	246.694	6.0134
[Pyr <sub>1,101</sub> ][NTf <sub>2</sub> ] [15]	276.791	6.6060	[Pyr <sub>1,4</sub> ][NTf <sub>2</sub> ] [16]	302.875	6.3880

( $\beta/10^{-4} \text{K}^{-1}$ ) of [Pyr<sub>1,101</sub>][FSA], [Pyr<sub>1,101</sub>][NTf<sub>2</sub>],<sup>15</sup> [Pyr<sub>1,4</sub>][FSA], and [Pyr<sub>1,4</sub>][NTf<sub>2</sub>]<sup>16</sup> at 298.15 K. [Pyr<sub>1,101</sub>][FSA] has the smallest molar volumes in the present ILs followed by [Pyr<sub>1,4</sub>][FSA], [Pyr<sub>1,101</sub>][NTf<sub>2</sub>], and [Pyr<sub>1,4</sub>][NTf<sub>2</sub>]. The volumetric changes with temperature for the ILs with the [Pyr<sub>1,101</sub>]<sup>+</sup> cation and [NTf<sub>2</sub>]<sup>-</sup> anion are more sensitive than those of the corresponding counterparts; i.e., [Pyr<sub>1,4</sub>]<sup>+</sup> < [Pyr<sub>1,101</sub>]<sup>+</sup> in a fixed anion and [FSA]<sup>-</sup> < [NTf<sub>2</sub>]<sup>-</sup> in a fixed cation. The temperature dependencies of the densities, viscosities, and electrical conductivities for the present ILs have not been reported, except for the viscosities and electrical conductivities of [Pyr<sub>1,4</sub>][FSA].<sup>2</sup>

The viscosities ( $\eta/\text{mPa}\cdot\text{s}$ ), electrical conductivities ( $\kappa/\text{S}\cdot\text{m}^{-1}$ ), and molar conductivities ( $\Lambda/\mu\text{S}\cdot\text{m}^2\cdot\text{mol}^{-1} (\equiv \kappa/c = \kappa M/\rho)$ ) for the two ILs are listed in Tables 1 and 2. The temperature dependencies of viscosities and electrical conductivities are presented in the Supporting Information (Figures S2 and S3). Each property was fitted to the Vogel–Fulcher–Tammann (VFT) equation:

$$\eta, \kappa, \text{ or } \Lambda = A' \exp(B/(T - T_0)) \quad (3)$$

and the Litovitz equation:

$$\mu, \kappa, \text{ or } \Lambda = A' \exp(B'/(RT^3)) \quad (4)$$

The coefficients of eq 3 ( $A$ ,  $B$ , and  $T_0$ ) and eq 4 ( $A'$  and  $B'$ ) are given in Table 4 with the Angell strength parameter  $D (= B/T_0)$ . The deviations from the Litovitz equations are smaller than the estimated experimental uncertainties, except for the viscosities in high-temperature extremes (see Figure 2 for viscosity and Figure 3 for electrical conductivity). On the other hand, the residuals between the experimental data and the calculated values from the VFT equations are smaller than 1 % over the temperature range of the present study. The squares of the correlation coefficients,  $R^2$ , for the VFT equations are very close to unity. The viscosities of [Pyr<sub>1,4</sub>][FSA] agree with the literature values at 293.15 K,<sup>2,4</sup> although they are a little higher than those reported by Zhou and co-workers<sup>2</sup> at higher temperatures as shown in Supporting Information (Figure S4). The electrical conductivities of [Pyr<sub>1,4</sub>][FSA] measured in the present study are higher than the previous values<sup>2,4</sup> (Figure S5). It is currently unclear what caused such deviations. One of the possibilities might be differences in experimental procedures. The replacement of the [NTf<sub>2</sub>]<sup>-</sup> anion with the [FSA]<sup>-</sup> anion decreases the viscosities and increases the conductivities as previously reported.<sup>1–4</sup> [Pyr<sub>1,101</sub>][FSA] has much lower viscosities and higher electrical conductivities than [Pyr<sub>1,4</sub>][FSA], and similar effects caused by the introduction of the ether group have been observed elsewhere.<sup>18–20</sup> The improvements in the transport properties are attributable to a more flexible methoxymethyl group with a smaller volume than the butyl group. The Angell strength parameter is also smaller in the fragile [Pyr<sub>1,101</sub>][FSA] than that in [Pyr<sub>1,4</sub>][FSA] (Table 4),

**Table 4. Coefficients of the Best Fits for Equations 3 and 4 for the Viscosities  $\eta$ , Electrical Conductivities  $\kappa$ , and Molar Conductivities  $\Lambda$**

		$\eta$		$\kappa$		$\Lambda$	
		mPa·s		$\text{S}\cdot\text{m}^{-1}$		$\mu\text{S}\cdot\text{m}^2\cdot\text{mol}^{-1}$	
[Pyr <sub>1,101</sub> ][FSA] eq 3	ln A	-1.52 <sub>8</sub>	(0.02 <sub>7</sub> )	4.11 <sub>5</sub>	(0.01 <sub>0</sub> )	9.72 <sub>3</sub>	(0.01 <sub>2</sub> )
	B	810. <sub>8</sub>	(9. <sub>5</sub> ) K	-617. <sub>5</sub>	(3. <sub>3</sub> ) K	-666. <sub>5</sub>	(3. <sub>8</sub> ) K
	$T_0$	132. <sub>0</sub>	(1. <sub>0</sub> ) K	146. <sub>9</sub>	(0. <sub>4</sub> ) K	142. <sub>9</sub>	(0. <sub>5</sub> ) K
	$D^\alpha$	6.14 <sub>3</sub>	(0.11 <sub>9</sub> )	-4.20 <sub>4</sub>	(0.03 <sub>4</sub> )	-4.66 <sub>4</sub>	(0.04 <sub>3</sub> )
	standard error of fit/%	0.19		0.08		0.09	
[Pyr <sub>1,101</sub> ][FSA] eq 4	ln A'	0.354 <sub>4</sub>	(0.017 <sub>1</sub> )	2.74 <sub>3</sub>	(0.00 <sub>3</sub> )	8.21 <sub>3</sub>	(0.00 <sub>8</sub> )
	B'/R	7.91 <sub>3</sub>		-7.17 <sub>9</sub>		-7.36 <sub>6</sub>	
		(0.04 <sub>8</sub> )·10 <sup>7</sup>		(0.01 <sub>4</sub> )·10 <sup>7</sup> K <sup>3</sup>		(0.02 <sub>2</sub> )·10 <sup>7</sup> K <sup>3</sup>	
	standard error of fit/%	1.61		0.43		0.65	
	[Pyr <sub>1,4</sub> ][FSA] eq 3	ln A	-1.70 <sub>2</sub>	(0.01 <sub>8</sub> )	4.20 <sub>7</sub>	(0.02 <sub>3</sub> )	9.91 <sub>7</sub>
B	905. <sub>2</sub>	(6. <sub>2</sub> ) K	-685. <sub>1</sub>	(7. <sub>2</sub> ) K	-730. <sub>8</sub>	(7. <sub>3</sub> ) K	
$T_0$	138. <sub>7</sub>	(0. <sub>6</sub> ) K	152. <sub>0</sub>	(0. <sub>8</sub> ) K	148. <sub>6</sub>	(0. <sub>8</sub> ) K	
$D^\alpha$	6.52 <sub>7</sub>	(0.07 <sub>3</sub> )	-4.50 <sub>8</sub>	(0.07 <sub>1</sub> )	-4.91 <sub>8</sub>	(0.07 <sub>6</sub> )	
standard error of fit/%	0.13		0.18		0.16		
[Pyr <sub>1,4</sub> ][FSA] eq 4	ln A'	0.362 <sub>0</sub>	(0.015 <sub>1</sub> )	2.72 <sub>6</sub>	(0.00 <sub>3</sub> )	8.30 <sub>7</sub>	(0.00 <sub>3</sub> )
	B'/R	9.55 <sub>3</sub>		-8.50 <sub>2</sub>		-8.68 <sub>1</sub>	
		(0.04 <sub>2</sub> )·10 <sup>7</sup>		(0.00 <sub>7</sub> )·10 <sup>7</sup> K <sup>3</sup>		(0.01 <sub>2</sub> )·10 <sup>7</sup> K <sup>3</sup>	
	standard error of fit/%	1.41		0.20		0.37	

<sup>α</sup>Angell strength factor ( $D = B/T_0$ ).

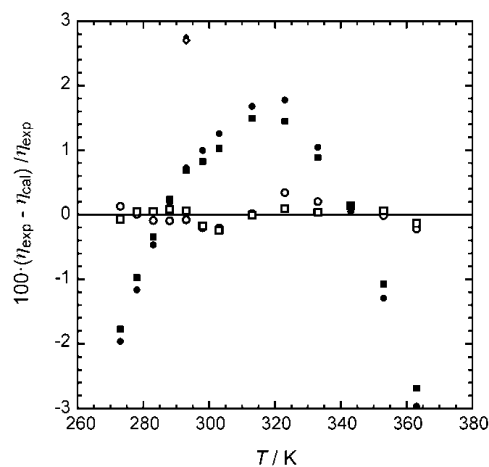


**Figure 2.** Residuals between the experimental viscosity  $\eta_{\text{exp}}$  and the calculated viscosity  $\eta_{\text{cal}}$  as a function of temperature  $T$ . Circle (open), [Pyr<sub>1,101</sub>][FSA] for VFT; circle (filled), [Pyr<sub>1,101</sub>][FSA] for Litovitz; square (open), [Pyr<sub>1,4</sub>][FSA] for VFT; square (filled), [Pyr<sub>1,4</sub>][FSA] for Litovitz; diamond (filled), [Pyr<sub>1,4</sub>][FSA] (ref 4) for VFT; diamond (open), [Pyr<sub>1,4</sub>][FSA] (ref 2) for VFT. Some data points in ref 2 were out of range (details are shown in the Supporting Information, Figure S4).

while [Pyr<sub>1,101</sub>][FSA] shows the larger Angell strength parameter than [Pyr<sub>1,101</sub>][NTf<sub>2</sub>].<sup>15</sup>

An empirical Walden product is useful to understand the relation between the viscosities and the electrical conductivities:

$$\Lambda \eta^\alpha = C \quad (5)$$

where  $\alpha$  is an adjustable parameter and  $C$  is a constant.<sup>21–24</sup> Figure 4 shows the logarithmic plots of molar conductivity versus

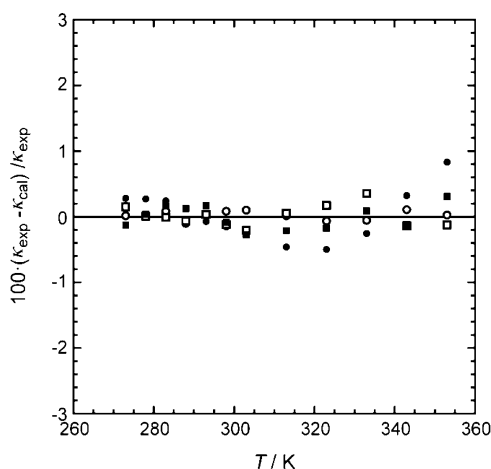


**Figure 3.** Residuals between the experimental electrical conductivity  $\kappa_{\text{exp}}$  and the calculated electrical conductivity  $\kappa_{\text{cal}}$  as a function of temperature  $T$ . Circle (open),  $[\text{Pyr}_{1,101}][\text{FSA}]$  for VFT; circle (filled),  $[\text{Pyr}_{1,101}][\text{FSA}]$  for Litovitz; square (open),  $[\text{Pyr}_{1,4}][\text{FSA}]$  for VFT; square (filled),  $[\text{Pyr}_{1,4}][\text{FSA}]$  for Litovitz. Data points in refs 2 and 4 were out of range (details are shown in the Supporting Information, Figure S5).

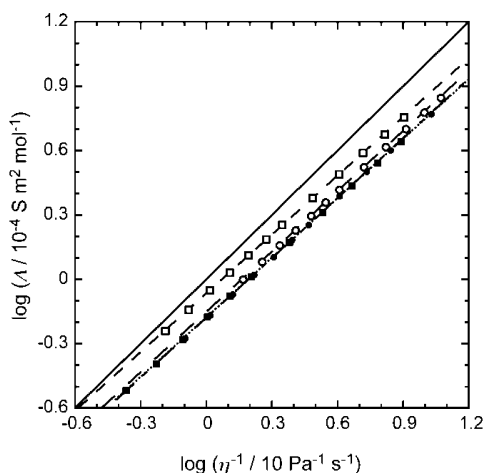


**Figure 4.** Logarithmic projection of the molar conductivity  $\Lambda$  – the fluidity (the reciprocal viscosity)  $\eta^{-1}$ . Circle (filled),  $[\text{Pyr}_{1,101}][\text{NTf}_2]$  (ref 15); circle (open),  $[\text{Pyr}_{1,101}][\text{FSA}]$ ; square (filled),  $[\text{Pyr}_{1,4}][\text{NTf}_2]$  (ref 16); square (open),  $[\text{Pyr}_{1,4}][\text{FSA}]$ . The solid line represents the Walden line with  $\alpha = 1$  and  $\log C = 0$ , and the dashed and dotted lines are eye guides.

fluidity (reciprocal viscosity). The slope and intercept correspond to  $\alpha$  and  $\log C$  in eq 5, respectively: they are found to be 0.937 and  $-0.154$  for  $[\text{Pyr}_{1,101}][\text{FSA}]$  and 0.913 and  $-0.067$  for  $[\text{Pyr}_{1,4}][\text{FSA}]$ . The values of  $\alpha$  and  $C$  are available for similar analogues with a different anion,  $[\text{NTf}_2]^-$ : 0.930 and  $-0.182$  for  $[\text{Pyr}_{1,101}][\text{NTf}_2]$ ,<sup>15</sup> 0.924 and  $-0.180$  for  $[\text{Pyr}_{1,4}][\text{NTf}_2]$ .<sup>16</sup> The slopes in the four ILs are smaller than unity, as generally observed in other ILs,<sup>20–23</sup> which indicates that the conductive flows of ions relatively decrease (increase) with increasing (decreasing) temperature from the expected values of fluidity.

Angell et al. have pointed out that the data points of “good ILs” are closer to the ideal line ( $\alpha = 1$ ,  $C = 0$ ) than those of “poor ILs” in the Walden plots.<sup>22</sup>  $[\text{Pyr}_{1,4}][\text{FSA}]$  is a so-called “good IL” and obviously shows better conductivity at a given fluidity than  $[\text{Pyr}_{1,4}][\text{NTf}_2]$  as well as the other ILs studied in the present work, though the absolute value of conductivity for  $[\text{Pyr}_{1,4}][\text{FSA}]$  is smaller at a fixed temperature than that for

$[\text{Pyr}_{1,101}][\text{FSA}]$ . The replacement of  $[\text{NTf}_2]^-$  by  $[\text{FSA}]^-$  effectively improves the Walden relation in  $[\text{Pyr}_{1,4}]^+$ . Interestingly, however, this is not the case for  $[\text{Pyr}_{1,101}]^+$ . Structural investigations such as vibrational and diffraction experiments and molecular simulations could provide meaningful information about the present specific results in the ether functionalized cation,  $[\text{Pyr}_{1,101}]^+$ .

## CONCLUSION

The densities, viscosities, and electrical conductivities of  $[\text{Pyr}_{1,101}][\text{FSA}]$  and  $[\text{Pyr}_{1,4}][\text{FSA}]$  have been measured at atmospheric pressure and at  $T = (273.15 \text{ to } 363.15) \text{ K}$ . Quadratic equations reproduce the densities of the present ILs within the deviations less than 0.005 %. Both the VFT and the Litovitz equations were successfully applied to fit the viscosities, the electrical conductivities, and the molar conductivities. The deviations between the calculated values from the VFT equations and the experimental data are less than 1 %. The Walden plots ( $\log \Lambda$  vs  $\log \eta^{-1}$ ) give the straight lines with slopes of 0.91 to 0.94, which are similar to values found for other ILs. ILs with the  $[\text{FSA}]^-$  anion show better transport properties (lower viscosity and higher electrical conductivity) than ILs with the  $[\text{NTf}_2]^-$  anion. The introduction of the ether group remarkably increases/decreases the conductivity/viscosity in  $N$ -alkyl- $N$ -methylpyrrolidinium ILs.

## ASSOCIATED CONTENT

### Supporting Information

Temperature dependencies of the experimental density (Figure S1), viscosity (Figure S2), and electrical conductivity (Figure S3) and overview of the residuals between experimental and calculated viscosity (Figure S4) and electrical conductivity (Figure S5). This material is available free of charge via the Internet at <http://pubs.acs.org>.

## AUTHOR INFORMATION

### Corresponding Author

\*E-mail: [m-kanakubo@aist.go.jp](mailto:m-kanakubo@aist.go.jp); fax: +81-22-232-7002.

### Funding

This work was partially supported by a Sasagawa Scientific Grant of the Japan Science Society and the Industrial Technology Research Grant Program in 2007 from the New Energy and Industrial Technology Development Organization (NEDO) of Japan.

## ACKNOWLEDGMENTS

The authors (T.M., M.K., T.U.) would thank Dr. Ken R. Harris at University of New South Wales, Australian Defence Force Academy for his helpful discussion and Eriko Niitsuma for her assistance with the measurements in the present study.

## LIST OF SYMBOLS

$A, B, T_0$	coefficients in the VFT equation
$A', B'$	coefficients in the Litovitz equation
$C$	constant in the Walden product
$D$	Angell strength parameter ( $= B/T_0$ )
$M$	molecular weight [ $\text{kg}\cdot\text{mol}^{-1}$ ]
$R$	gas constant [ $\text{J}\cdot\text{mol}^{-1}\cdot\text{K}^{-1}$ ]
$T$	temperature [K]
$\alpha$	coefficient in the Walden product
$\eta$	viscosity [ $\text{Pa}\cdot\text{s}$ ]
$\kappa$	electrical conductivity [ $\text{S}\cdot\text{m}^{-1}$ ]
$\rho$	density [ $\text{kg}\cdot\text{m}^{-3}$ ]
$\Lambda$	molar conductivity [ $\text{S}\cdot\text{m}^2\cdot\text{mol}^{-1}$ ]



## REFERENCES

- (1) Matsumoto, H.; Sakaebe, H.; Tatsumi, K.; Kikuta, M.; Ishiko, E.; Kono, M. Fast cycling of Li/LiCoO<sub>2</sub> cell with low-viscosity ionic liquids based on bis(fluorosulfonyl)imide [FSI]<sup>-</sup>. *J. Power Sources* **2006**, *160*, 1308–1313.
- (2) Zhou, Q.; Henderson, W. A.; Appetecchi, G. B.; Montanino, M.; Passerini, S. Physical and Electrochemical Properties of N-Alkyl-N-methylpyrrolidinium Bis(fluorosulfonyl)imide Ionic Liquids: PY<sub>13</sub>FSI and PY<sub>14</sub>FSI. *J. Phys. Chem. B* **2008**, *112*, 13577–13580.
- (3) Hayamizu, K.; Tsuzuki, S.; Seki, S.; Fujii, K.; Suenaga, M.; Umebayashi, Y. Studies on the translational and rotational motions of ionic liquids composed of N-methyl-N-propyl-pyrrolidinium (P<sub>13</sub>) cation and bis(trifluoromethanesulfonyl)amide and bis(fluorosulfonyl)amide anions and their binary systems including lithium salts. *J. Chem. Phys.* **2010**, *133*, 194505.
- (4) Johansson, P.; Fast, L. E.; Matic, A.; Appetecchi, G. B.; Passerini, S. The conductivity of pyrrolidinium and sulfonylimide-based ionic liquids: A combined experimental and computational study. *J. Power Sources* **2010**, *195*, 2074–2076.
- (5) MacFarlane, D. R.; Meakin, P.; Sun, J.; Amini, N.; Forsyth, M. Pyrrolidinium Imides, A New Family of Molten Salts and Conductive Plastic Crystal Phases. *J. Phys. Chem. B* **1999**, *103*, 4164–4170.
- (6) Tokuda, H.; Tsuzuki, S.; Hasan Susan, Md. A. B.; Hayamizu, K.; Watanabe, M. How Ionic Are Room-Temperature Ionic Liquids? An Indicator of the Physicochemical Properties. *J. Phys. Chem. B* **2006**, *110*, 19593–19600.
- (7) Gardas, R. L.; Costa, H. F.; Freire, M. G.; Carvalho, P. J.; Marrucho, I. M.; Fonseca, I. M. A.; Ferreira, A. G. M.; Coutinho, J. A. P. Densities and Derived Thermodynamic Properties of Imidazolium-, Pyridinium-, Pyrrolidinium-, and Piperidinium-Based Ionic Liquids. *J. Chem. Eng. Data* **2008**, *53*, 805–811.
- (8) Appetecchi, G. B.; Montanino, M.; Zane, D.; Carewska, M.; Alessandrini, F.; Passerini, S. Effect of the alkyl group on the synthesis and the electrochemical properties of N-alkyl-N-methyl-pyrrolidinium bis(trifluoromethanesulfonyl)imide ionic liquids. *Electrochim. Acta* **2009**, *54*, 1325–1332.
- (9) Kanatani, T.; Ueno, R.; Matsumoto, K.; Nohira, T.; Hagiwara, R. Thermal properties of N-alkyl-N-methylpyrrolidinium and N-butylpyridinium fluorometallates and physicochemical properties of their melts. *J. Fluorine Chem.* **2009**, *130*, 979–984.
- (10) Harris, K. R.; Woolf, L. A.; Kanakubo, M. Temperature and Pressure Dependence of the Viscosity of the Ionic Liquid 1-Butyl-3-methylimidazolium Hexafluorophosphate. *J. Chem. Eng. Data* **2005**, *50*, 1777–1782.
- (11) Harris, K. R.; Kanakubo, M.; Woolf, L. A. Temperature and Pressure Dependence of the Viscosity of the Ionic Liquids 1-Methyl-3-octylimidazolium Hexafluorophosphate and 1-Methyl-3-octylimidazolium Tetrafluoroborate. *J. Chem. Eng. Data* **2006**, *51*, 1161–1167.
- (12) Harris, K. R.; Kanakubo, M.; Woolf, L. A. Temperature and Pressure Dependence of the Viscosity of the Ionic Liquids 1-Hexyl-3-methylimidazolium Hexafluorophosphate and 1-Butyl-3-methylimidazolium Bis(trifluoromethylsulfonyl)imide. *J. Chem. Eng. Data* **2007**, *52*, 1080–1085.
- (13) Kanakubo, M.; Harris, K. R.; Tsuchihashi, N.; Ibuki, K.; Ueno, M. Temperature and pressure dependence of the electrical conductivity of the ionic liquids 1-methyl-3-octylimidazolium hexafluorophosphate and 1-methyl-3-octylimidazolium tetrafluoroborate. *Fluid Phase Equilib.* **2007**, *261*, 414–420.
- (14) Kanakubo, M.; Harris, K. R.; Tsuchihashi, N.; Ibuki, K.; Ueno, M. Effect of pressure on transport properties of the ionic liquid 1-butyl-3-methylimidazolium hexafluorophosphate. *J. Phys. Chem. B* **2007**, *111*, 2062–2069.
- (15) Kanakubo, M.; Nanjo, H.; Nishida, T.; Takano, J. Density, viscosity, and electrical conductivity of N-methoxymethyl-N-methylpyrrolidinium bis(trifluoromethanesulfonyl)amide. *Fluid Phase Equilib.* **2011**, *302*, 10–13.
- (16) Harris, K. R.; Woolf, L. A.; Kanakubo, M.; Rütther, T. Transport Properties of N-butyl-N-methylpyrrolidinium Bis(trifluoromethylsulfonyl)amide. *J. Chem. Eng. Data* **2011**, *56*, 4672–4685.
- (17) Beran, M.; Příhoda, J. A New Method of the Preparation of Imido-bis(sulfuric acid) Dihalogenide, (F,Cl), and the Potassium Salt of Imido-bis(sulfuric acid) Difluoride. *Z. Anorg. Allg. Chem.* **2005**, *631*, 55–59.
- (18) Sato, T.; Maruo, T.; Marukane, S.; Takagi, K. Ionic liquids containing carbonate solvent as electrolytes for lithium ion cells. *J. Power Sources* **2004**, *138*, 253–261.
- (19) Zhou, Z.-B.; Matsumoto, H.; Tatsumi, K. Low-Melting, Low-Viscous, Hydrophobic Ionic Liquids: Aliphatic Quaternary Ammonium Salts with Perfluoroalkyltrifluoroborates. *Chem.—Eur. J.* **2005**, *11*, 752–766.
- (20) Ferrari, S.; Quartarone, E.; Mustarelli, P.; Magistris, A.; Protti, S.; Lazzaroni, S.; Fagnoni, M.; Albini, A. A binary ionic liquid system composed of N-methoxyethyl-N-methylpyrrolidinium bis-(trifluoromethanesulfonyl)imide and lithium bis(trifluoromethanesulfonyl)imide: A new promising electrolyte for lithium batteries. *J. Power Sources* **2009**, *194*, 45–50.
- (21) Xu, W.; Cooper, E. I.; Angell, C. A. Ionic Liquids: Ion Mobilities, Glass Temperatures, and Fragilities. *J. Phys. Chem. B* **2003**, *107*, 6170–6178.
- (22) Angell, C. A.; Byrne, N.; Belieres, J.-P. Parallel Developments in Aprotic and Protic Ionic Liquids: Physical Chemistry and Applications. *Acc. Chem. Res.* **2007**, *40*, 1228–1236.
- (23) Ueno, K.; Tokuda, H.; Watanabe, M. Ionicity in ionic liquids: correlation with ionic structure and physicochemical properties. *Phys. Chem. Chem. Phys.* **2010**, *12*, 1649–1658.
- (24) Wu, T.-Y.; Su, S.-G.; Lin, Y.-C.; Wang, H. P.; Lin, M.-W.; Gung, S.-T.; Sun, I.-W. Electrochemical and physicochemical properties of cyclic amine-based Brønsted acidic ionic liquids. *Electrochim. Acta* **2010**, *56*, 853–862.